

Physical properties of 6dF dwarf galaxies

Jean Michel Gomes and Polychronis Papaderos

Abstract Spectral synthesis is basically the decomposition of an observed spectrum in terms of the superposition of a base of simple stellar populations of various ages and metallicities, producing as output the star formation and chemical histories of a galaxy, its extinction and velocity dispersion.

The STARLIGHT code provides one of the most powerful spectral synthesis tools presently available. We have applied this code to the entire Six-Degree-Field Survey (6dF) sample of nearby star-forming galaxies, selecting dwarf galaxy candidates with the goal of

- deriving the age and metallicity of their stellar populations
- and creating a database with the physical properties of our sample galaxies together with the FITS files of pure emission line spectra (i.e. the observed spectra after subtraction of the best-fitting synthetic stellar spectrum).

Our results yield a good qualitative and quantitative agreement with previous studies based on the Sloan Digital Sky Survey (SDSS). However, an advantage of 6dF spectra is that they are taken within a twice as large fiber aperture, much reducing aperture effects in studies of nearby dwarf galaxies.

1 Introduction

We have entered in a new era with the availability of high-quality spectroscopic data bases for large galaxy samples, such as the Sloan Digital Sky Survey (SDSS) and Six-Degree Field (6dF) Surveys. The combination of a wide set of synthetic and observed stellar libraries with meanwhile much refined population synthesis codes permits us to significantly improve our understanding of the formation and evolution of galaxies.

One such publicly available code for the derivation of physical properties of galaxies is STARLIGHT [5]. The main output from the model, $M(\lambda)$, is a linear com-

Jean Michel Gomes and Polychronis Papaderos
CAUP - Centro de Astrofísica da Universidade do Porto
Rua das Estrelas, 4150-762 Porto, Portugal
e-mail: jean@astro.up.pt and papaderos@astro.up.pt

bination of N_* Simple Stellar Populations (SSPs) of different age and metallicity. This study uses Bruzual & Charlot SSP models [3]. The basic equation is:

$$\frac{M(\lambda)}{M(\lambda_0)} = \sum_{j=1}^{N_*} x_{j,\lambda_0} b_{j,\lambda_0}(\lambda) r(\lambda) \otimes G(v_*, \sigma_*) \quad (1)$$

where, $M(\lambda_0)$ is the flux of the best-fitting model at the normalization wavelength λ_0 , x_{j,λ_0} is the j^{th} SSP flux contribution at λ_0 to the modeled spectrum, $b_{j,\lambda_0}(\lambda)$ is the j^{th} SSP spectrum normalized at λ_0 , $r(\lambda)$ is the extinction law (Cardelli, Clayton, & Mathis [4]). $G(v_*, \sigma_*)$ is a Gaussian folding function that is used to take into account the stars' velocity dispersion σ_* and the systemic velocity v_* .

The principle by-product of this equation is the Star Formation History (SFH) encoded in the population vector expressed in terms of x_{j,λ_0} . Therefrom we derive the luminosity-weighted mean stellar age ($\langle \log t_* \rangle_L = \sum_{j=1}^{N_*} x_{j,\lambda_0} \log t_j$) and metallicity ($\langle Z_* \rangle_L = \sum_{j=1}^{N_*} x_{j,\lambda_0} Z_j$), where t_j and Z_j are the age and metallicity of the j^{th} SSP and secondary quantities, such as the Mass-to-Light (M2L) ratio in the K , H and J filters, which together with photometry, allows us to estimate the total stellar mass (M_*) of galaxies.

2 The 6dF Sample

We have studied the entire final data release of the 6dF Survey [6], which comprises spectra and K , H and J 2MASS photometry for 136 304 galaxies with a mean redshift of 0.053, much lower than that of SDSS. The spectra were obtained in two observations using separate V and R gratings, that together yield a resolution of ~ 1000 over the spectral range 4000–7500 Å and a signal-to-noise ratio ~ 10 per pixel. After a series of tests, we decided to model the V part of the spectrum only due to its better calibration, which is vital for a reliable derivation of the SFH with STARLIGHT. However, emission lines from both parts of the spectrum have been used to distinguish between star-forming galaxies and AGNs, based on the diagnostic emission-line ratios: $[\text{OIII}]\lambda 5007/\text{H}\beta$ and $[\text{NII}]\lambda 6583/\text{H}\alpha$ in BPT diagrams [2].

2.1 Dwarf Galaxy Candidates in the 6dF

After selecting spectral fits with a percentage deviation from input spectra of less than 5%, we extracted a sub-sample of $\sim 20\,000$ galaxies. This is the high-quality (HQ) sample, out of which we selected 116 dwarf galaxies by using a “soft” criterion that is based on the absolute K magnitude ($-20.5 \leq M_K \leq -13.5$; Fig. 1). 90 of these galaxies are star-forming.

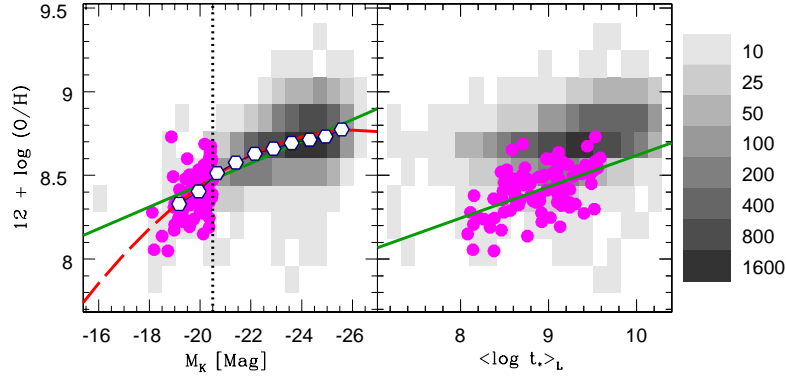


Fig. 1 Comparison of the subsample of 90 star-forming dwarf galaxies (filled magenta circles) with the entire High Quality (HQ) sample of star-forming galaxies (7938 objects) in the 6dF. The grey-scale distribution in the right bar depicts the number of galaxies in each bin. **Left panel:** Absolute K magnitude vs gas-phase metallicity. The vertical dotted line marks the absolute magnitude range of $-20.5 \leq M_K \leq -13.5$ adopted for the extraction of the dwarf galaxy sample. The solid and dashed lines show a linear and polynomial fit to the median trend shown with white hexagons. **Right panel:** Luminosity-weighted mean stellar age vs nebular metallicity for the HQ 6dF sample. A linear fit to the dwarf galaxy subsample (solid line) suggest a slight steepening of the stellar age vs metallicity relation for low-mass galaxies.

3 Results

We computed the nebular metallicity using the N2 index ($N2 \equiv \log [NII]\lambda 6583/H\alpha$) following the parametrization of Pettini & Pagel [8]. In Fig. 1 we show the absolute magnitude M_K vs the nebular metallicity (right panel). The dotted line marks the absolute magnitude range adopted for the selection of dwarf galaxies. The luminosity-weighted mean stellar age vs gas-phase metallicity for the dwarf galaxy candidates is shown on the right panel. We can see that dwarf galaxy candidates span ~ 2 dex with respect to $\langle \log t_* \rangle_L$ with systems among them harboring old stellar populations being predominantly metal-rich and *vice versa*.

An important outcome from this study is outlined in Fig. 2 where we show the stellar mass–nebular metallicity (MZ) relation, and the stellar mass and gas-phase metallicity distributions for the entire HQ sample and the sub-sample of the 90 dwarf galaxy candidates. The MZ relation, as derived from the SDSS DR7 data is included for comparison. The dwarf galaxy candidates, whose median stellar mass and nebular metallicity is by, respectively, ~ 2 and ~ 0.3 dex lower than the values determined for the entire HQ data set, follow the overall trend found for star-forming galaxies, independently corroborating previous studies ([7, 9, 1], among others). A follow-up analysis and discussion of the MZ relation, based on 6dF data is planned in [10].

Acknowledgements J. M. Gomes is supported by a Post-Doctoral grant, funded by FCT/MCTES (Portugal) and POPH/FSE (EC) and P. Papaderos is supported by Ciencia 2008 Contract, funded by FCT/MCTES (Portugal) and POPH/FSE (EC).

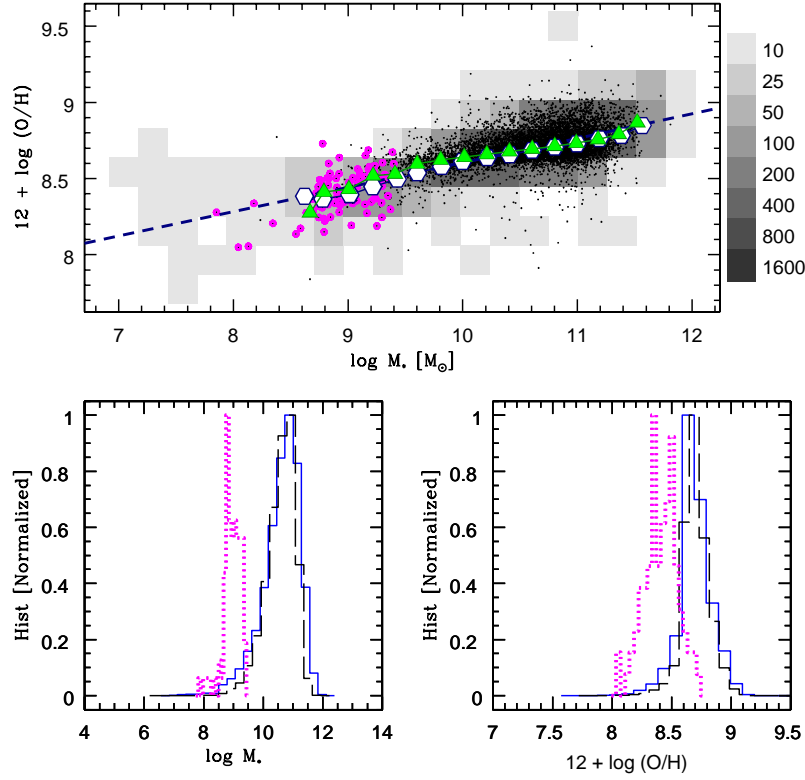


Fig. 2 **Top panel:** Stellar mass vs nebular metallicity (MZ) relation for the 6dF HQ sample (black dots) and the dwarf galaxy sub-sample (filled circles). For comparison, we show the SDSS DR7 sample with a grey-scale distribution, representing the number of galaxies in each pixel (vertical bar). The median trend is shown with green triangles and white hexagons for the 6dF and SDSS DR7 sample, respectively. Linear fits to both 6dF and SDSS galaxies (dashed line) are practically identical, independently confirming previous results (e.g.: Tremonti et al. 2004). **Bottom Panels:** Histograms with the stellar mass (left) and the gas-phase metallicity (right) of the HQ and dwarf galaxy sample from the 6dF, and from the SDSS (dotted, dashed and solid lines, respectively).

References

1. Asari et al. 2009, MNRAS, 396L, 71
2. Baldwin J. A., Phillips M. M., Terlevich R., PASP, 93, 5
3. Bruzual G., Charlot S. 2003, MNRAS, 344, 1000
4. Cardelli et al. 1989, ApJ, 345, 245
5. Cid Fernandes et al. 2005, MNRAS, 358, 363
6. Jones et al. 2009, MNRAS, 399, 683
7. Lequeux J. et al. 1979, A&A, 80, 155
8. Pettini M., Pagel B. 2004, MNRAS, 348L, 59
9. Tremonti C. A. et al. 2004, ApJ, 613, 898
10. Gomes, J.-M. & Papaderos, P. 2011, in prep.